

KASCADE-Grande energy spectrum of cosmic rays and the role of hadronic interaction models

M. BERTAINA³, W.D. APEL¹, J.C. ARTEAGA-VELÁZQUEZ², K. BEKK¹, J. BLÜMER^{1,4}, H. BOZDOG¹, I.M. BRANCUS⁵, E. CANTONI^{3,6,a}, A. CHIAVASSA³, F. COSSAVELLA^{4,b}, C. CURCIO³, K. DAUMILLER¹, V. DE SOUZA⁷, F. DI PIERRO³, P. DOLL¹, R. ENGEL¹, J. ENGLER¹, B. FUCHS⁴, D. FUHRMANN^{8,c}, H.J. GILS¹, R. GLASSTETTER⁸, C. GRUPEN⁹, A. HAUNGS¹, D. HECK¹, J.R. HÖRANDEL¹⁰, D. HUBER⁴, T. HUEGE¹, K.-H. KAMPERT⁸, D. KANG⁴, H.O. KLAGES¹, K. LINK⁴, P. ŁUCZAK¹¹, M. LUDWIG⁴, H.J. MATHES¹, H.J. MAYER¹, M. MELISSAS⁴, J. MILKE¹, B. MITRICA⁵, C. MORELLO⁶, J. OEHLISCHLÄGER¹, S. OSTAPCHENKO^{1,d}, N. PALMIERI⁴, M. PETCU⁵, T. PIEROG¹, H. REBEL¹, M. ROTH¹, H. SCHIELER¹, S. SCHOO¹, F.G. SCHRÖDER¹, O. SIMA¹², G. TOMA⁵, G.C. TRINCHERO⁶, H. ULRICH¹, A. WEINDL¹, J. WOCHOLE¹, J. ZABIEROWSKI¹¹

KASCADE-GRANDE COLLABORATION

¹ Institut für Kernphysik, KIT - Karlsruher Institut für Technologie, Germany

² Universidad Michoacana, Instituto de Física y Matemáticas, Morelia, Mexico

³ Dipartimento di Fisica, Università degli Studi di Torino, Italy

⁴ Institut für Experimentelle Kernphysik, KIT - Karlsruher Institut für Technologie, Germany

⁵ National Institute of Physics and Nuclear Engineering, Bucharest, Romania

⁶ Osservatorio Astrofisico di Torino, INAF Torino, Italy

⁷ Universidade São Paulo, Instituto de Física de São Carlos, Brasil

⁸ Fachbereich Physik, Universität Wuppertal, Germany

⁹ Department of Physics, Siegen University, Germany

¹⁰ Dept. of Astrophysics, Radboud University Nijmegen, The Netherlands

¹¹ National Centre for Nuclear Research, Department of Cosmic Ray Physics, Lodz, Poland

¹² Department of Physics, University of Bucharest, Bucharest, Romania

^a now at: Istituto Nazionale di Ricerca Metrologica, INRIM, Torino;

^b now at: Max-Planck-Institut Physik, München, Germany;

^c now at: University of Duisburg-Essen, Duisburg, Germany;

^d now at: University of Trondheim, Norway.

bertaina@to.infn.it

Abstract: Previous results obtained by KASCADE-Grande using QGSjetII-02 hadronic interaction model have shown that the energy spectrum of cosmic rays between 10^{16} eV and 10^{18} eV exhibits a hardening at $\sim 2 \times 10^{16}$ eV and a slight but statistically significant steepening at $\sim 10^{17}$ eV, caused by the heavy component of primary cosmic rays. In this paper, we report on results of similar analyses performed using SIBYLL 2.1, EPOS 1.99 and QGSjetII-04 hadronic interaction models to interpret the data. The present results confirm the previous findings. The intensity of the all-particle spectrum, the locations of the hardening and the steepening of the spectrum, as well as the relative abundance of the heavy and light mass groups depend on the hadronic interaction model.

Keywords: KASCADE-Grande, Air Showers, hadronic interaction models, mass composition, energy spectrum

1 Introduction

The recent findings of KASCADE-Grande [1, 2, 3] indicate that there are some features in the all-particle energy spectrum and in the spectra of the mass-groups in the energy range 10^{16} - 10^{18} eV. Such findings rely on the results of simulations and the description of hadronic interactions for reconstructing the properties of the primary particle which differ in predictions. Therefore, a cross-check of the results obtained with various interaction models will help in understanding the systematic effects of this kind.

In this paper, we present the results on the all-particle energy spectrum and mass-group separation of KASCADE-Grande data interpreted using the SIBYLL 2.1 [4], EPOS 1.99 [5], and QGSjetII-04 [6] high-energy hadronic interaction models in the CORSIKA framework [7], and compare them to the previous findings obtained using QGSjetII-02. The technique to infer the energy spectrum and mass separation is the same as in the QGSjetII-02 analyses [1, 2, 3] and it is described in detail in [8]. In the

following, the names are abbreviated as SIBYLL, EPOS, QGS2v4 (for QGSjetII-04) and QGSjet (for QGSjetII-02), respectively. In all cases, FLUKA [9] is used to describe the low-energy interactions in air-shower development.

2 The technique

The technique employed to derive the all-particle energy spectrum and the abundance of ‘light’ and ‘heavy’ primaries is based on the correlation between the number of charged particles (N_{ch}) with energy $E > 3$ MeV, and muons (N_{μ}) with kinetic energy $E > 230$ MeV on an event-by-event basis. Grande stations provide the core position and angle-of-incidence, as well as the total number of charged particles in the shower at observation level. The values are calculated by means of a maximum likelihood procedure comparing the measured number of particles with the one expected from a modified NKG lateral distribution function. The total number of muons is calculated us-

ing the core position determined by the Grande array and the muon densities measured by the KASCADE muon array detectors. Also in this case the total number of muons N_μ in the shower disk is derived from a maximum likelihood estimation where the lateral distribution function is based on the one proposed by [10]. The reconstruction procedures and accuracies of KASCADE-Grande observables are described in detail in [11] and related references therein.

Sets of simulated events were produced in the energy range from 10^{15} eV to 3×10^{18} eV with high statistics and for five elements: H, He, C, Si and Fe, representative for different mass groups.

For the reconstruction of experimental events and simulated data, we restricted ourselves to events with zenith angles less than 40° . Additionally, only air showers with cores located in a central area of the KASCADE-Grande array were selected (~ 0.15 km²). With these cuts on the fiducial area, border effects are discarded and possible under- and overestimations of the muon number for events close to and far away from the center of the KASCADE array are reduced. All of these cuts were applied also to the Monte Carlo simulations to study their effects. Full efficiency for triggering and reconstruction of air-showers is reached at a primary energy of $\approx 10^{16}$ eV. The analysis presented here is finally based on 1173 days of data taking and the cuts on the sensitive central area and zenith angle correspond to a total acceptance of $A = 0.1976$ km² sr, and an exposure of $N = 0.635$ km² sr year, respectively.

Based on Monte Carlo simulations a formula is obtained to calculate the primary energy per individual shower on the basis of the reconstructed N_{ch} and N_μ . The formula takes into account the mass sensitivity in order to minimize the composition dependence in the energy assignment, and at the same time, provides an event-by-event separation between ‘light’ and ‘heavy’ candidates. The formula is defined for 5 different zenith angle intervals independently, to take into account shower attenuation in the atmosphere. Data are combined only at the very last stage to obtain a unique power law spectrum. The energy assignment is defined as $E = f(N_{ch}, k)$ (see equation 1), where N_{ch} is the number of charged particles and the parameter k is defined through the ratio of the numbers of the N_{ch} and N_μ components: $k = g(N_{ch}, N_\mu)$ (see equation 2). The main aim of the k variable is to take into account the average differences in the N_{ch}/N_μ ratio among different primaries with similar N_{ch} and the shower to shower fluctuations for events of the same primary mass :

$$\log_{10} E = [a_H + (a_{Fe} - a_H) \cdot k] \cdot \log_{10} N_{ch} + b_H + (b_{Fe} - b_H) \cdot k \quad (1)$$

$$k = \frac{\log_{10}(N_{ch}/N_\mu) - \log_{10}(N_{ch}/N_\mu)_H}{\log_{10}(N_{ch}/N_\mu)_{Fe} - \log_{10}(N_{ch}/N_\mu)_H} \quad (2)$$

$$\log_{10}(N_{ch}/N_\mu)_{H,Fe} = c_{H,Fe} \cdot \log_{10} N_{ch} + d_{H,Fe} \cdot d_{H,Fe}. \quad (3)$$

The k parameter is, by definition of eq. (2), a number centered around 0 for H initiated showers and 1 for Fe ones if expressed as a function of N_{ch} for Monte Carlo events. It is expected that the average values of the k parameter for the experimental data lie between the H and Fe limits. In case this is not verified it would be a hint of some deficit of the model to describe the experimental data. Naturally, as the calibration functions differ from model to model, the same experimental event might give different values of k when different calibration functions are used.

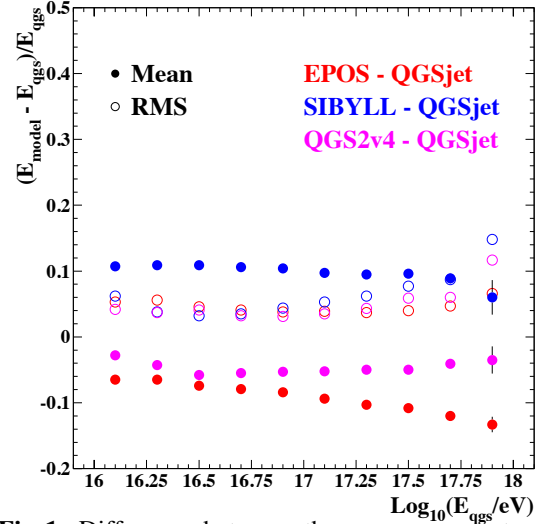


Fig.1: Difference between the energy reconstructed by SIBYLL (filled blue dots), EPOS (filled red dots), or QGS2v4 (filled pink dots) on experimental data compared to QGSjet as a function of the energy reconstructed by QGSjet. The open dots refer to the width of the distributions in each energy bin.

Simulated events using a mixture of all primaries have been divided in bins of true energy and the distributions of the relative differences between reconstructed and true energies have been created. The RMS of such distributions (energy resolution) is $\sim 26\%$ at the energy threshold and decreases with energy, due to the lower fluctuations of the shower development and reconstruction uncertainties, becoming $< 20\%$ at the highest energies. The ratio of the reconstructed flux over the true one in each energy differs by less than 10% from unity. This results applies also for pure light (50% H - 50% He) or pure heavy (50% Si - 50% Fe) compositions. A similar behavior exists for all hadronic interaction models.

Assuming QGSjet as the reference model for a fixed energy, SIBYLL simulated events show less amount of electrons and muons, while EPOS and QGS2v4 a higher muon content. As a consequence, when interpreting the same experimental event, SIBYLL is expected to assign a higher energy than QGSjet, while EPOS and QGS2v4 a lower one. This is confirmed by fig.1, which shows the average relative difference between the energy reconstructed by SIBYLL, EPOS and QGS2v4 compared to QGSjet on an event-by-event basis, for different energy bins. SIBYLL assigns on average a 10% higher energy than QGSjet at all energies, while QGS2v4 and EPOS lower ones by $\sim 5\%$ and $\sim 10\%$, respectively .

3 The energy spectrum

Applying the energy calibration functions obtained by each model to the measured data, the all-particle energy spectra for the five zenith angle bins are obtained for QGSjet, SIBYLL, EPOS and QGS2v4. For all the models, except QGS2v4, an unfolding procedure has been applied as well. Different sources of uncertainty affect the all-particle energy spectrum. A detailed description is reported in [2]. They take into account: a) the angular dependence of the param-

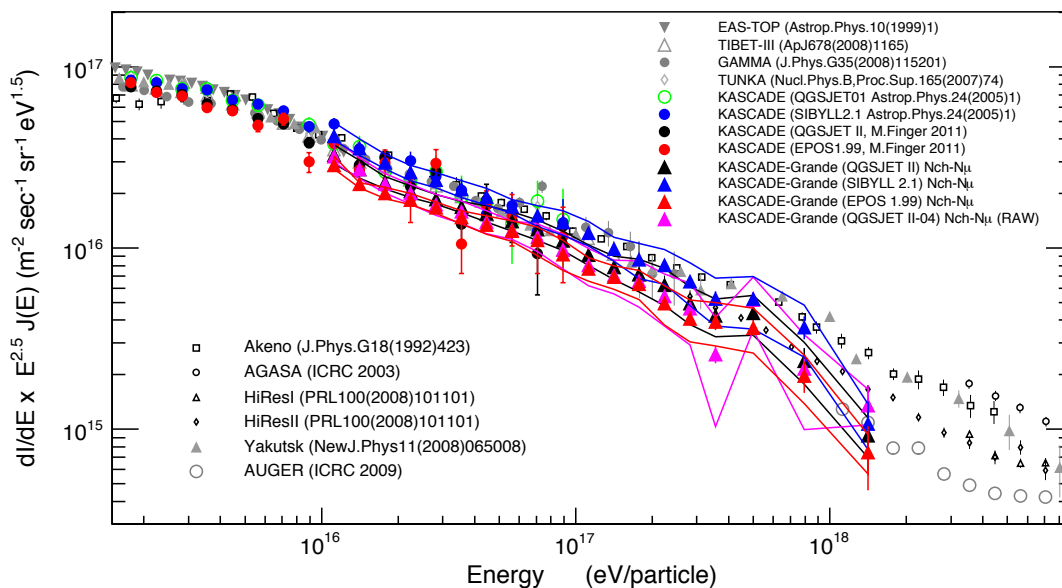


Fig. 2: Comparison of the all-particle energy spectrum obtained with KASCADE-Grande data based on SIBYLL (blue), QGSJet (black), QGS2v4 (pink) and EPOS (red) models to results of other experiments. The band denotes the systematic uncertainties in the flux estimation.

eters appearing in the energy calibration functions of the different angular ranges. b) The possible bias introduced in the energy spectrum by different primary compositions. c) The spectral slope of Monte Carlo used in the simulations. d) The reconstruction quality of N_{ch} and N_{μ} . The total systematic uncertainty is $\sim 20\%$ at the threshold ($E = 10^{16}$ eV) and $\sim 30\%$ at the highest energies ($E = 10^{18}$ eV) almost independently from the interaction model used to interpret the data. The final all-particle spectrum of KASCADE-Grande is obtained (see Fig. 2) by combining the spectra for the individual angular ranges. Only those events are taken into account, for which the reconstructed energy is above the energy threshold for the angular bin of interest. In general the shape of the energy spectrum is very similar for the three models, however, a shift in flux is clearly observed which amounts to $\sim 25\%$ increase in case of SIBYLL and $\sim 10\%$ decrease in case of EPOS. This is the consequence of the energy shift assigned on an event-by-event basis previously discussed. This result gives an estimation on the systematic uncertainty on the experimental flux due to the hadronic interaction model used to interpret the data, and it is essentially independent of the technique used to derive the flux, namely averaging the fluxes obtained in different angular bins. The shift in the assigned energy to the data is also visible in the hardening around $\sim 2 \times 10^{16}$ eV and in the steepening around 10^{17} eV which look shifted among the models in general agreement with the energy shift. This result indicates that the features seen in the spectrum are not an artefact of the hadronic interaction model used to interpret the data but they are in the measured data. In the overlapping region, KASCADE-Grande data are compatible inside the systematic uncertainties with KASCADE data interpreted with the same model.

4 The separation into mass groups

The mass-group separation is performed subdividing the measured data in samples, defined as ‘heavy’ and ‘light’ mass-groups based on the k parameter - see equation 2. A detailed explanation of the procedure is reported in [1, 3]. The analysis is conducted independently for each hadronic interaction model. In each energy bin the average value of k for pure H, He, C, Si and Fe simulated compositions is evaluated. These values are very similar among models by construction (see equation 2). In fact H showers will lead to average k values close to 0 and Fe showers close to 1. Two lines are used to separate events into heavy ($k(E) > k_h(E)$) and light mass groups ($k(E) < k_l(E)$), where the separation line of the heavy mass-group is defined by fitting the $k_h(E) = (k_{Si}(E) + k_C(E))/2$ points which are obtained by averaging the values of k for Si and C components of the simulated events, and the light mass-group is defined by fitting the $k_l(E) = (k_C(E) + k_{He}(E))/2$ points which are obtained by averaging the values of k for C and He components of the simulated events. Naturally, the absolute abundances of the experimental data in the two samples depend on the location of the straight lines. However, the evolution of the abundances as a function of energy will be retained by this approach, as the lines are defined through a fit to the k values. The assignment to the heavy or light mass groups is performed on an event-by-event basis. Due to the different N_{ch}/N_{μ} ratio among models for the same k value, the same experimental event might be assigned to the same group, to none of them or even to a different group depending on the model used. As a consequence, the abundances of the so defined heavy and light groups will vary among models. Fig. 3 shows the abundances of the heavy (left plot) and of the light (right plot) according to the different hadronic interaction models used to interpret the data. With such a selection cut the reconstructed spectrum of the heavy primary sample shows

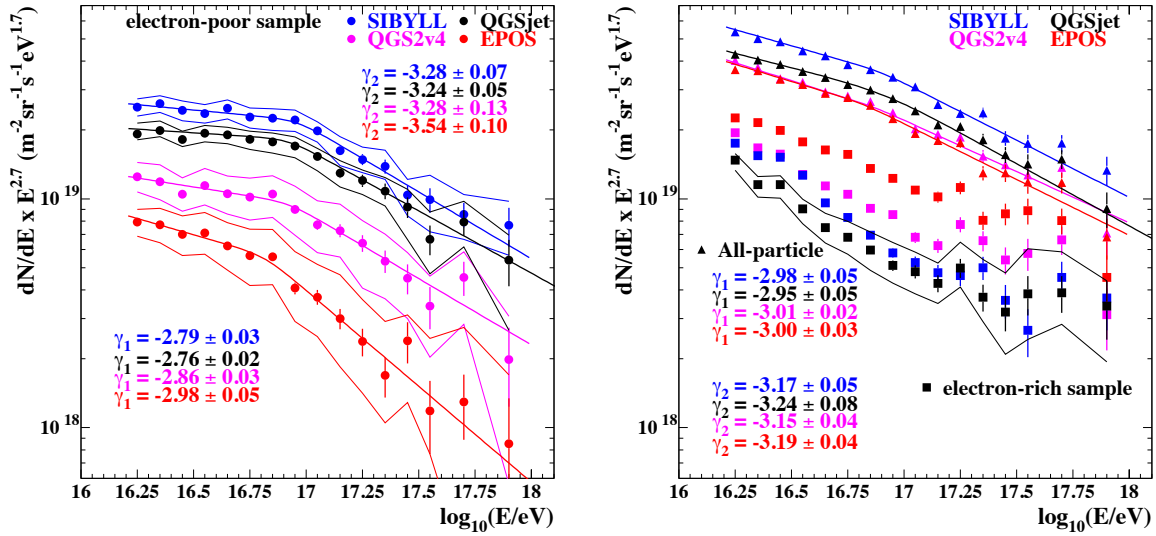


Fig. 3: Reconstructed energy spectra of the heavy (left plot) and light components together with the all-particle spectrum (right plot) for the four hadronic interaction models. The error bars show the statistical uncertainties; the bands assign systematic ones due to the selection of subsamples. For the light component only the systematic uncertainties of QGSjet have been indicated, anyhow they are similar in all models. Fits on the spectra and resulting slopes are also indicated.

Table 1: Slope of the different spectra and break positions obtained with the four different hadronic interaction models, by applying the k parameter analysis in order to extract the spectrum of the heavy component.

| Model | EPOS | QGS2v4 | QGSjet | SIBYLL |
|----------------------|------------------|------------------|------------------|------------------|
| All-part. | | | | |
| γ_1 | -3.00 ± 0.03 | -3.01 ± 0.02 | -2.95 ± 0.05 | -2.98 ± 0.05 |
| γ_2 | -3.19 ± 0.04 | -3.15 ± 0.04 | -3.24 ± 0.08 | -3.17 ± 0.05 |
| $\log(E/eV)$ | 16.82 ± 0.09 | 16.88 ± 0.20 | 16.92 ± 0.10 | 16.90 ± 0.12 |
| signif. (σ) | 2.8 | 1.7 | 2.1 | 2.7 |
| Heavy c. | | | | |
| γ_1 | -2.98 ± 0.05 | -2.86 ± 0.03 | -2.76 ± 0.02 | -2.79 ± 0.03 |
| γ_2 | -3.54 ± 0.10 | -3.28 ± 0.13 | -3.24 ± 0.05 | -3.28 ± 0.07 |
| $\log(E/eV)$ | 16.82 ± 0.07 | 16.92 ± 0.09 | 16.92 ± 0.04 | 16.96 ± 0.04 |
| signif. (σ) | 4.0 | 2.4 | 3.5 | 7.4 |

a distinct knee-like feature around 10^{17} eV for all hadronic interaction models. Applying a fit of two power laws to the spectrum interconnected by a smooth knee in the entire energy range $16.2 < \log_{10}(E/eV) < 18.0$ results in a statistical significance that the entire spectrum cannot be fitted with a single power-law. These results are summarized in tab.1. The spectrum of the electron-rich component is much steeper with a possible hardening at the highest energies for all models. Details are discussed in [3, 12].

5 Conclusions

The energy spectrum and separation into mass-groups have been obtained for SIBYLL, EPOS and QGS2v4 hadronic interaction models using the same approach defined for QGSjet in [1, 2, 3]. The results - see [13] for details - confirm qualitatively the previous findings. The all-particle spectrum in the range $10^{16} - 10^{18}$ eV is found to exhibit some smaller structures: In particular, a hardening of the spectrum at $\sim 2 \times 10^{16}$ eV, a small break-off at $\sim 8 \times 10^{16}$ eV. The energy position of such features slightly depends on the energy assigned by the interaction model to the event. In general is at lower energies for EPOS and QGS2v4 and higher energies for QGSjet and SIBYLL. The separation into mass groups performed via the k parameter re-

veals that the knee-like feature around 10^{17} eV in the all-particle spectrum is associated with a break in the heavy component. The abundance of the heavy component varies significantly among models. In this sense the interpretation of which mass group is responsible for this break strongly depends on the hadronic interaction model employed to interpret the data.

The all-particle spectra of KASCADE-Grande are in good agreement with those obtained by KASCADE.

Acknowledgment: The authors would like to thank the members of the engineering and technical staff of the KASCADE-Grande collaboration, who contributed to the success of the experiment. The KASCADE-Grande experiment is supported in Germany by the BMBF and by the Helmholtz Alliance for Astroparticle Physics - HAP funded by the Initiative and Networking Fund of the Helmholtz Association, by the MIUR and INAF of Italy, the Polish Ministry of Science and Higher Education, and the Romanian Authority for Scientific Research UEFISCDI (PNII-IDEI grants 271/2011 and 17/2011).

References

- [1] W.-D. Apel et al. - KASCADE-Grande Coll., Phys. Rev. Lett. 107 (2011) 171104.
- [2] W.-D. Apel et al. - KASCADE-Grande Coll., Astrop. Phys. 36 (2012) 183-194.
- [3] W.-D. Apel et al. - KASCADE-Grande Coll., Phys. Rev. D 87 (2013) 081101.
- [4] J. Engel et al., Phys. Rev. D 46 (1992) 5013-5025.
- [5] K. Werner et al., Phys. Rev. C 74 (2006) 044902/1-11.
- [6] S. Ostapchenko, Phys. Rev. D 74 (2006) 014026/1-17.
- [7] D. Heck et al., FZKA6019 (1998).
- [8] M. Bertagna et al. - KASCADE-Grande Coll., Astroph. and Space Science Trans. 7 (2011) 229-234.
- [9] G. Battistoni et al., AIP Conf. Proc. 896 (2007) 31-49.
- [10] A.-A. Lagutin et al., Nucl. Phys. B (Proc. Suppl.) 97 (2001) 274-277.
- [11] W.-D. Apel et al. - KASCADE-Grande Coll., Nucl. Instr. Meth. Phys. Res., Sect. A 620 (2010) 202-216.
- [12] S. Schöo et al. - KASCADE-Grande Coll., these proceedings #0527.
- [13] W.-D. Apel et al. - KASCADE-Grande Coll., accepted at Advan. in Space Res. (2013), doi:10.1016/j.asr.2013.05.008.